Synthesis of Boron Nitride Nanotubes by a Template-Assisted Polymer Thermolysis Process

ARTICLE *in* THE JOURNAL OF PHYSICAL CHEMISTRY C · FEBRUARY 2007

Impact Factor: 4.77 · DOI: 10.1021/jp074178k · Source: OAI

Synthesis of Boron Nitride Nanotubes by a Template-Assisted Polymer Thermolysis Process

Mikhael Bechelany,[†] Samuel Bernard,*[,†] Arnaud Brioude,[†] David Cornu,[†] Pierre Stadelmann,[‡] Catherine Charcosset,[§] Koffi Fiaty,[§] and Philippe Miele[†]

Laboratoire des Multimateriaux et Interfaces (UMR CNRS 5615), Université Lyon1, Université de Lyon, 43 bd du 11 Novembre 1918, 69622 Villeurbanne Cedex, France, Interdepartemental Centre of Electron Microscopy, CIME, Swiss Federal Institute of Technology, EPFL, CH-1015 Lausanne, Switzerland, and Laboratoire d'Automatique et de Génie des procédés (UMR CNRS 5007), CPE - Université Lyon1, Université de Lyon, 43 bd du 11 Novembre 1918, 69622 Villeurbanne Cedex, France

Received: May 30, 2007; In Final Form: July 5, 2007

Highly ordered arrays of boron nitride nanotubes (BN-NTs) were prepared for the first time by combining a polymer thermolysis route and a template process. The strategy involves four steps, i.e., synthesis of a liquid polymeric borazine, liquid-phase infiltration of an alumina membrane, thermolysis at 1200 °C under nitrogen of the polymer confined in the 200 nm ordered nanochannels, and template etching to generate BN-NTs arrays supported by a BN sheet. Their crystallinity was controlled through further high-temperature treatments. The thin multiwall BN-NTs displaying dimensions corresponding to the pore size were characterized by electron microscopies and electron energy loss spectroscopy. It was demonstrated that the formation of nanotubes was governed by evaporation of low molecular weight species during the initial steps of the thermolysis, causing loss of nanowire integrity, while a thin film remained and covered the pore walls as a result of the high surface energy of the alumina mold.

Introduction

The past decade has seen an increasing demand for the preparation of one-dimensional (1D) inorganic nanostructures including nanotubes and nanowires in various phases and compositions.[1−5] Such nanostructured materials displaying novel physical and chemical properties have great potential in a wide variety of application going from optoelectronic nanodevices to composite materials.[6−12] Among such materials, boron nitride nanotubes (BN-NTs) are paid special attention as alternatives to conventional carbon nanotubes (CNTs) as a result of the structural similarity between *h*-BN and graphite. BN nanotubes are even thought to be more amenable than carbon nanotubes for a number of applications including gas adsorption, electron transport, field emission measurements, and composite structural material. In particular, BN-NTs are predicted to have interesting electronic properties insensitive to tube diameters, and their resistance toward oxidation up to 700 °C in air represents a significant advantage over carbon nanotubes which readily oxidize at 400 °C.[13]

There are currently numerous routes for the synthesis of BN nanotubes like chemical vapor deposition, arc-discharge, and laser-ablation methods,[14−18] but only a few techniques allow production of aligned BN NTs with a narrow size distribution despite their potential applications in engineering materials as, for instance, in nanocomposites.

The possibility to assemble individual nanotubes into a special arrangement for preparing ordered arrays of nanotubes with controlled diameter, length, and density could arise from the membrane-assisted template process. The templating process historically introduced by Possin et al.[19] helps to prepare many kinds of highly ordered arrays of 1D nanoscale objects including organic polymers, carbon, metals, and metal oxide systems when combining with chemical approaches such as electrodeposition, chemical vapor deposition (CVD), and sol−gel techniques.[20−27] In the case of the membrane-assisted template process, the technique involves nanoporous anodic aluminum oxide (AAO) membranes as inorganic templates containing a large number of straight cylindrical pores with a narrow size distribution. Arrays of monodispersed and highly ordered nanowires or nanotubes are shaped by filling the nanochannels with the desired material in the gas or liquid phase. The diameter, length, and density of 1D nanostructures are ideally determined by the size, depth, and interval of pores in AAO templates. To the best of our knowledge, only a membrane-assisted template process coupled with a CVD approach was used to prepare ordered arrays of BN nanotubes.[28] However, these processes are usually very complex and require heavy equipment which drastically increase the cost of the resulting nanostructures in the case of industrial application. In addition, the density and quality of the as-obtained nanotubes closely depend on the efficiency of the gas-filling process and usually require a relatively long infiltration time.

In our work, the strategy used to prepare BN-NTs can overcome these limitations to a certain extent. It is based on a liquid-phase infiltration (LPI) process through the combination of the templating process and the polymer thermolysis route. Using the general polymer thermolysis route,[29−31] a large variety of net-shaped non-oxide ceramics, i.e., polymer-derived ceramics (PDCs), can be built up from molecular units and shaped by controlling the structure of the molecular units as well as the polymerization and thermolysis procedures. Interestingly, the

* To whom correspondence should be addressed. E-mail: Samuel.Bernard@univ-lyon1.fr. Tel.: +33 472 433 612. Fax: +33 472 440 618.

[†] Laboratoire des Multimateriaux et Interfaces, Université Lyon1.

[‡] Swiss Federal Institute of Technology.

[§] Laboratoire d'Automatique et de Génie des procédés, Université Lyon1.

10.1021/jp074178k CCC: $37.00
Published on Web 08/21/2007

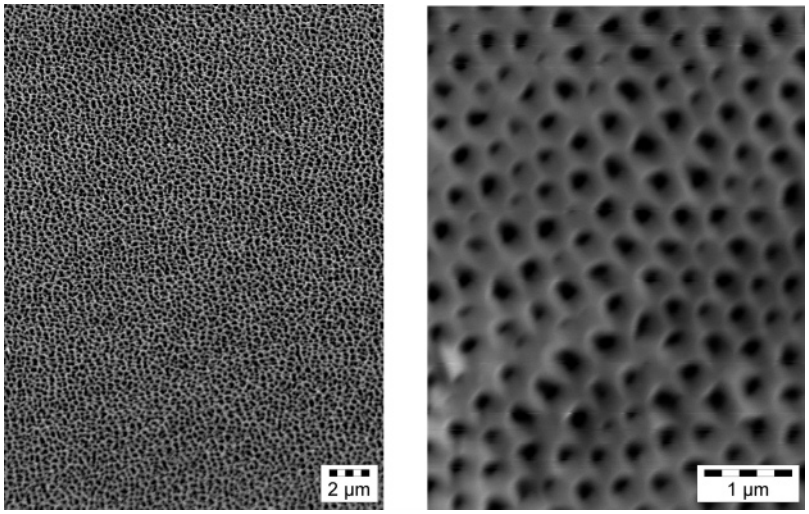

Figure 1. SEM images of the as-received AAO membrane.

direct polymer thermolysis route makes polymers compatible with many shaping techniques such as infiltration offering the opportunity to realize complex shapes/structures in a simple and cost-efficient way. The general concept combining the templating process and the polymer thermolysis route consists of the synthesis of non-gaseous molecular precursors and their polymerization into preceramic polymers which filled the nanochannels of a membrane in the liquid phase to generate a panel of green nanowires. The latter undergo heat treatment to be converted into highly ordered 1D ceramic nanostructures including nanowires or nanotubes. Relevant research with respect to this template-assisted liquid polymer approach is quite limited.[32−33] Sneddon et al. investigated the preparation of boron carbide nanowires by infiltation of an organoborane melt inside porous alumina membranes.[32] In a same approach, Interrante et al.[33] prepared hollow 1D silicon carbide nanostructures from liquid carbosilanes. In all cases, the polymer-to-ceramic conversion was followed by acid or base treatment to remove the alumina matrix and recover the corresponding ceramic material, i.e., boron carbide and silicon carbide. To the best of our knowledge, the synthesis of boron nitride nanotube arrays using the LPI method from preceramic polymers has not yet been demonstrated.

Herein, and following our works developed in the group of Si- and B-based nanowires and nanocables,[5,34,35] multiwall BN-NTs have been successfully prepared for the first time by a liquid thermolysis process combined with porous AAO templates. We demonstrate that infiltration of a commercial AAO template with a synthesized liquid polymeric borazine to form the green nanowires followed by their thermolysis in the confined space to produce the ceramic phase leads to highly ordered BN-NT arrays connected on a surface side by a boron nitride sheet, which grows on the surface of AAO closely. A plausible model for the understanding of the formation of such 1D nanostructures is proposed. The production of such nanotubes after heat-treatment at high temperature was confirmed by high-resolution transmission electron microscopy (HRTEM) and electron energy loss spectroscopy (EELS). The BN-NTs that we have prepared are observed to have a thin tube wall thickness along the entire length of the nanotube. The fabrication procedure of BN-NTs can be regarded as a model for fabrication of nanotubes of other types of non-oxide ceramics through LPI and polymer thermolysis processes.

Experimental Details

Materials. Syntheses were carried out in an argon atmosphere, using argon/vacuum lines, and Schlenk-type flasks. Argon (>99.995%) was purified by passing through successive columns of phosphorus pentoxide, siccapent, and BTS catalysts. Schlenks were dried at 120 °C overnight before pumping under vacuum and filling them with argon for synthesis and infiltration. The alumina template membrane used was a commercially available filter (Anodizc 47 from Whatman) that was 60 μm thick and had a nominal 200 nm pore diameter (Figure 1).

Sodium borohydride ($NaBH_4$, ≥98.5%, powder from Sigma-Aldrich), ammonium sulfate ($(NH_4)_2SO_4$, ≥99.0% from Sigma-Aldrich), and tetraethylene glycol dimethyl ether ($CH_3O(CH_2CH_2O)_4CH_3$, 99% from Sigma-Aldrich) were used to prepare the borazine molecule.

Manipulation of the chemical products was made inside an argon-filled glove box (Jacomex BS521) dried with phosphorus pentoxide.

Polymer Synthesis. In a 2 L Schlenk flask, equipped with a water reflux condenser and a magnetic stirrer, 82 g (2.167 mol) of $NaBH_4$ and 372 g (2.815 mol) of $(NH_4)_2SO_4$ were carefully dissolved in 800 mL of tetraethylene glycol dimethyl ether at room temperature (RT). A BH_4^-/NH_4^+ molar ratio of 0.385 was fixed. Under vigorous stirring, the reaction mixture was carefully heated under controlled vacuum to 120 °C, and the borazine was continuously removed as it is formed and recovered through a series of three traps which were put in liquid nitrogen at the exit of the reflux condenser. A hold time of 2 h 30 min was maintained at 120 °C to achieve the reaction. Borazine was distilled under reduced pressure by trap-to-trap, and the colorless liquid retained in the last trap was in final transferred under reduced pressure toward a Schlenk which was placed in liquid nitrogen. Borazine (43.5 g, 53.2% relative to $NaBH_4$) was used without further purification. It should be mentioned that elemental analysis cannot be performed due to the poor thermal stability of borazine at RT.

IR (CsI windows/cm^{-1}): ν(N−H) = 3451 m; ν(B−H) = 2509 m,; ν(B−N) = 1454 s; δ(B−N−B) = 897 m. ^{1}H NMR (300 MHz/$CDCl_3$/ppm): δ = 3.6−5.8 (quadruplet, 3H, B*H*), 5.3−5.9 (triplet, 3H, N*H*). ^{11}B NMR (96.29 MHz/C_6D_6/ppm): δ = 30.1 (br).

For the following thermolysis step, 16.2 g of the as-obtained borazine were introduced in a 75 mL pressurized system at P_{Ar} = 1 bar. Borazine was heated to 50 °C (5 °C min^{-1}) creating

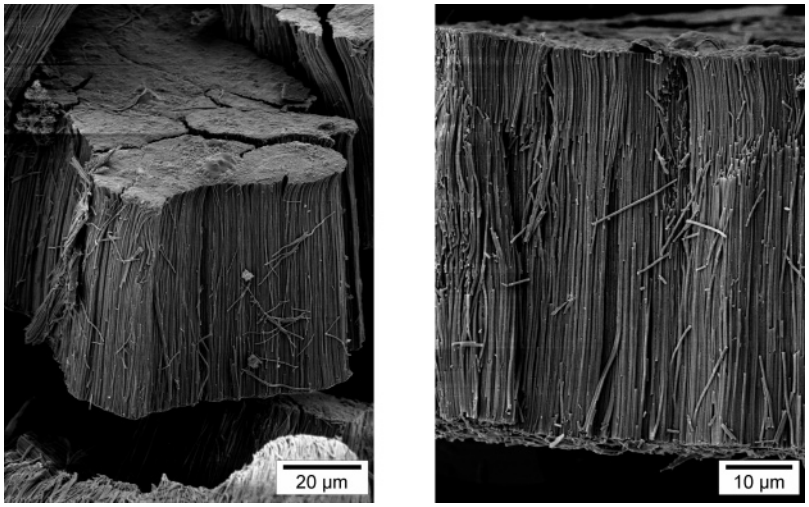

Figure 2. SEM images of close-packed arrays of aligned 1D nanostructures obtained at 1200 °C. Samples were sputter-coated with Pd/Au to reduce charging.

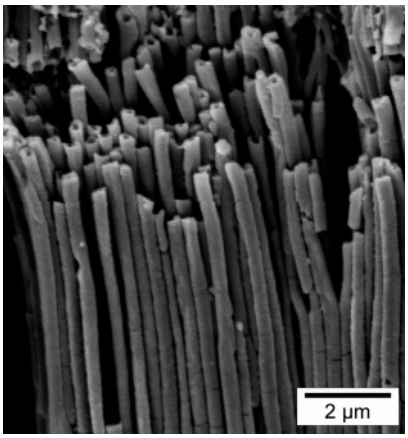

Figure 3. SEM image of the back side of the membrane showing nanotubes obtained at 1200 °C.

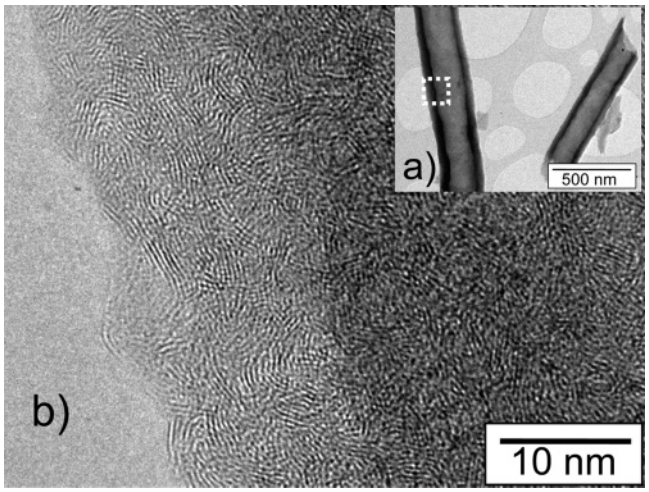

Figure 4. (a) TEM images of nanotubules produced at 1200 °C. (b) HRTEM observation of the stacking ordering (zone marked by the dotted square in the TEM image).

an internal pressure of 30.1 bar at the end of the thermolysis step (dwell time of ~192 h). After the mixture was cooled down to RT, a colorless liquid (14.1 g, 87%) was delivered. It was stable at RT for several weeks.

Anal. Found: B, 36.2; N, 59.3; H, 4.5 $[B_{3.0}N_{3.8}H_{4.0}]_n$ ($[89.69]_n$). IR (CsI windows/cm^{-1}): ν(N−H) = 3451 m; ν(B−H) = 2509 m; ν(B−N) = 1441 s; δ(B−N−B) = 901 m. ^{1}H NMR (300 MHz/$CDCl_3$/ppm): δ = 3.4−5.1 (quadruplet, B*H*), 5.1−5.9 (triplet, N*H*). ^{11}B NMR (96.29 MHz/C_6D_6/ppm): δ = 30.2 (br). TGA (N_2, 1000 °C, 46.8% ceramic yield): 25−180 °C: Δm = 48%; 180−1000 °C: Δm = 5.2%.

Nanotube Preparation. Infiltration was made on pieces of alumina membrane with an area of ~1 cm^2 placed in an alumina boat inside a 500 mL Schlenk flask in an argon atmosphere. Before LPI, pieces of membrane were dried at 120 °C for 96 h and subsequently pumped under vacuum inside the Schlenk flask. The polymeric borazine was deposed on the surface of pieces at RT with a 1 mL syringe. The number of LPI cycles required for completely wetting each AAO membrane varied between 2 and 4. After absorption and formation of a film covering the membranes, the Schlenk-type glass containing the impregnated pieces of membrane was heated uniformly to 200 °C in an oil bath and held at this temperature for 2 h. Finally, the system was allowed to cool to RT under constant flow (50 mL min^{-1}) of argon, and the as-received composites were then transferred into an alumina tube inserted in a horizontal tube furnace (Vecstar Furnace model VTF 7). The tube was pumped under vacuum and refilled with nitrogen (99.995%). Subsequently, samples were subjected to a cycle of ramping of 1 °C min^{-1} to 1200 °C, dwelling there for 2 h, and then cooling down to RT at 5 °C min^{-1}. A constant flow (120 mL min^{-1}) of nitrogen was passed through the tube. Then, the AAO template embedded with BN-NTs were immersed in 48% hydrofluoric acid for 96 h at RT in PTFE systems, then washed thoroughly with deionized water, methanol, and acetone to completely remove the alumina. For heating above 1200 °C, samples free of alumina were placed in boron nitride boats, then introduced in a graphitic furnace (Gero model HTK 8) which was subsequently pumped then refilled with nitrogen to be heated through a cycle of ramping of 2 °C min^{-1} to the desired temperature between 1450 and 1800 °C, dwelling there for 2 h, and then cooling down to RT at 5 °C min^{-1}. A constant flow (200 mL min^{-1}) of nitrogen was passed through the furnace.

Characterization. Thermogravimetric analysis (TGA) of the polymer-to-ceramic conversion was recorded on a Setaram TGA 92 16.18. Experiments were performed in a nitrogen atmosphere at 1 °C min^{-1} from RT to 1000 °C using silica crucibles (sample weight of ~40 mg) at ambient atmospheric pressure. Experimental differential thermogravimetric (DTG) data were generated from TGA measurements. The as-prepared BN-NTs were characterized and analyzed by a Hitashi S800 scanning electron

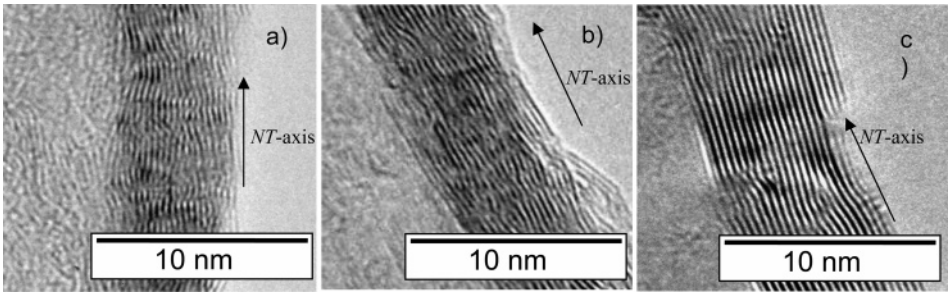

Figure 5. HRTEM images of the stacking ordering of the BN layers after heating to (a) 1450, (b) 1600, and (c) 1800 °C.

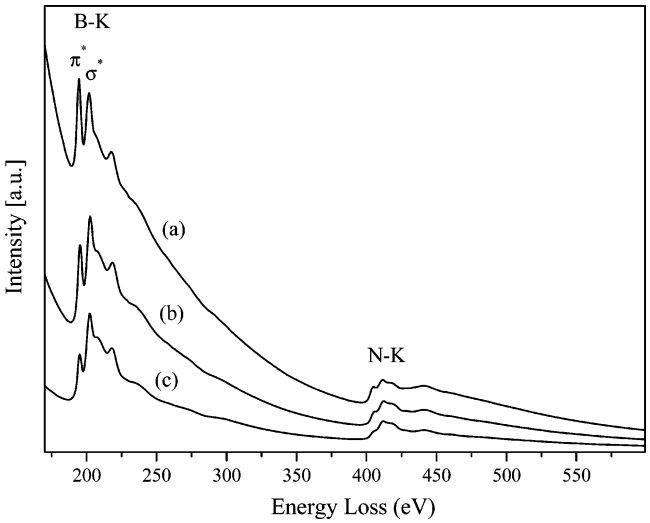

Figure 6. EELS spectrum of BN nanotubes produced at 1800 °C going from the outer surface (a) to the center (c) of nanotubes.

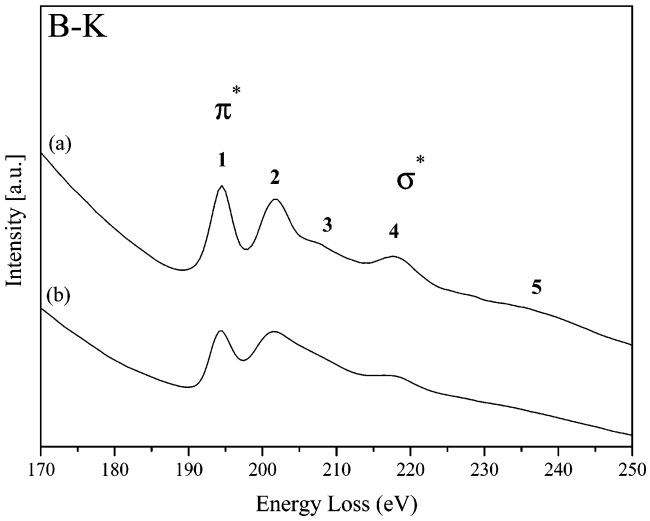

Figure 7. Fine structure of the B K edges for BN nanotubes produced from the liquid polymeric borazine at 1800 (a) and 1200 °C (b).

microscopy (SEM) and a transmission electron microscopy (TEM) with a TOPCON 002B at each final temperature: 1200, 1450, 1600, and 1800 °C. For SEM observations, samples were mounted on stainless pads and, due to their insulating properties, they were sputtered with ~10 Å of a Pd/Au mixture to prevent charging during observation. The chemical analyses were performed by electron energy loss spectroscopy (LGatan PEELS model 666) during the HRTEM analyses. This EELS study was conducted in the line-scan mode by moving the electron probe along a segment perpendicular to the nanotube axis.

Results and Discussion

Borazine has been used as BN molecular precursor. It was prepared similarly to the procedure developed by Sneddon et al. starting from $NaBH_4$ and $(NH_4)_2S0_4$.[36] Referring to its chemical formula $H_3B_3N_3H_3$ and structure, borazine represents a source of both boron and nitrogen elements with the correct boron-to-nitrogen ratio and symmetry. In addition, it offers the advantage of being a liquid compound, suggesting to us that it can be used to generate 1D BN nanostructures using LPI and thermolysis processes. Unfortunately, borazine is unstable at RT and has a tendency to completely evaporate during the further ceramic conversion by heat treatment. This fact prevents the preparation of 1D nanostructures by direct heat treatment of borazine. Thus, the key step to produce 1D BN nanostructures is to control the thermal reactivity of borazine allowing it to be shaped (processability, e.g., liquid or fusible) in the alumina mold in a stable process, then transformed into BN by heat treatments without full evaporation (ceramic yield). Our strategy by which this can be accomplished is to polymerize the borazine into a RT stable liquid polymer before infiltration. It is indeed possible to polymerize the borazine at low temperature inside a pressure-sealed system. A 75 mL pressurized device was loaded with 20 mL of borazine at 0 °C in an argon atmosphere and heated to 50 °C (5 °C min^{-1}) to carry out polymerization. Temperature was maintained at 50 °C, creating relatively high pressure within the vessel due to the release of hydrogen from borazine. Thermolysis was stopped when the internal pressure did not increase anymore (~192 h), and the temperature was thus allowed to cool down to RT to generate a colorless liquid ($[B_{3.0}N_{3.8}H_{4.0}]_n$; oxygen values were found to be lower than 2 atom % and were therefore omitted). NMR and FT-IR experiments confirmed that thermolysis proceeded through ring condensation forming naphthalene-like derivatives and hydrogen release (NH and BH absorption bands decreased in intensity, and the sharp B−N absorption at 1454 cm^{-1} changed to a broad absorption band at 1441 cm^{-1}), giving a borazine-based polymer which is found to be stable at RT for several weeks. It has to be mentioned that the term "polymer" is used in its broad sense, that is, as a group of molecules whose structure can be generated through repetition of a few elementary borazine units.

The liquid polymer was deposed at RT in flowing argon on the surface of pieces of AAO membranes placed in alumina boats inside a Schlenk-type glass. After absorption of the polymer into the nanochannels of the porous alumina, infiltration was repeated until saturation of the membrane and formation of a thin liquid film covering it. The impregnated pieces of membranes were subsequently heated in the Schlenk flask up to 200 °C under argon and held at this temperature for 2 h to enable the solidification of the polymer confined in the nanochannels of the membrane. After they were cooled to RT, the as-received pieces of membrane were recovered by a thin transparent solid film. The pieces made of the thermoset polymer in the nanochannels and the alumina template were next introduced into a tubular furnace to be subjected to a solid state thermolysis

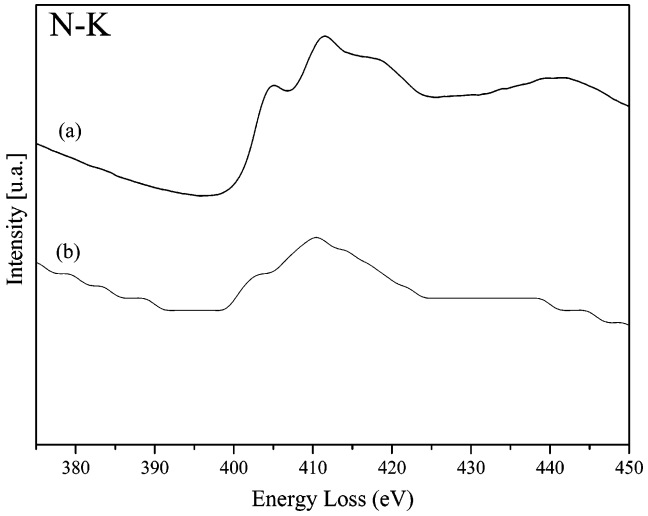

Figure 8. Fine structure of the N K edges for BN nanotubes produced from the liquid polymeric borazine at 1800(a) and 1200 °C (b).

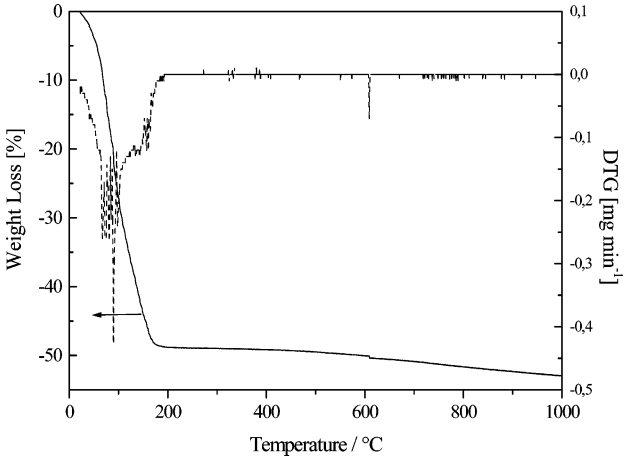

Figure 9. TG and DTG (square symbols) curves of the liquid polymer. Nitrogen atmosphere up to 1000 °C (1 °C min^{-1}).

at 1200 °C in a nitrogen atmosphere (1 °C min^{-1}, dwell time of 2 h) yielding white pieces of ceramic-filled membranes. Then, the templates embedded with the expected ceramic were immersed in a solution of 48% hydrofluoric acid for 96 h at RT to remove alumina and were washed thoroughly with deionized water, methanol, and acetone. The morphology of the as-synthesized samples was observed with scanning electron microscopy (SEM, Figure 2).

Figure 2 shows that the preorganization of the liquid polymer in the nanoscale channels of the membranes followed by the annealing of the composite to 1200 °C, then membrane destruction creates a close-packed array of aligned and monodispersed nanowires supported by a thin film. No residual alumina was observed after membrane dissolution, which was supported by complementary FT-IR and XRD analyses: samples were characterized before and after membrane dissolution, and as-obtained spectra were compared to conclude on the absence of alumina. The density of these nanoobjets demonstrates the efficiency of the LPI process for high-yield preparation. In addition, the formation of ~60 μm long 1D nanostructures indicates complete filling of the template during the LPI process. The SEM image (Figure 3) of the back side of a part of the membrane shown in Figure 2 allows us to unambiguously prove that these parallel and straight defect-free nanowires are hollow. The as-produced nanotubes show a uniform diameter of 200 nm, which matches that of the template nanochannels. It should be mentioned that the preparation of vertical nanotube arrays are reproducibly accomplished by filling, then saturing the AAO membrane during the LPI process.

Although the wall thickness is distributed in a large range going from 5 to 50 nm, a majority of nanotubes exhibits a wall thickness of 10−20 nm along the entire length of the nanotube (Figure S1 in Supporting Information).

The low-magnification TEM bright field image (Figure 4, inset) reveals that the BN-NT produced at 1200 °C is a straight nanotube with an average diameter of 200 nm.

The corresponding HRTEM image of a wall part (Figure 4) shows that the structure of nanotubes produced at 1200 °C is nanocrystalline and lamellar with layers significantly buckled in a disordered stacking sequence. Nanograins exhibit a size around 5 atomic basal planes and lengths of <50 Å indicating the formation of a poorly crystallized BN phase.

Studies of the polymer-derived ceramics, and in particular polyborazine-derived boron nitride, have demonstrated that the crystallinity level and crystalline quality of these materials is mainly controlled by the final temperature of the process.[37−39] Therefore, to improve the nanostructural ordering of the BN phase, nanotubes underwent further heat treatments up to 1800 °C in a nitrogen atmosphere. SEM studies demonstrated that the annealing of as-produced nanotubes at 1450, 1600, and 1800 °C changed their microscopic feature (SEM, Figure S2 in Supporting Information). Their surface becomes rough when annealing to 1800 °C, suggesting that crystallization occurs in the temperature range 1200−1800 °C. Investigations of similar wall areas by HRTEM after heat treatments of nanotubes at 1450, 1600, and 1800 °C (Figure 5) gave a clear representation of the post-thermolysis development of the BN nanostructural ordering and confirmed SEM suggestions. It should be mentioned that only nanotubes with low wall thickness (~8 nm) were selected for HRTEM analysis in order to obtain highly resolved images.

When the thermal treatment is conducted above 1200 °C (dwell time of 2 h at each applied temperature), the relatively high tortuosity in the stacking sequence of the layers gradually disappears. The nanomaterials obtained at 1800 °C even show distinctly ordered wall structures demonstrating the significant improvement in the stacking order of layers. These high-quality crystalline nanostructures even can implausibly form the usual tubular morphologies of multiwalled BN nanotubes. The wall consists of a relatively large amount of stacked 002 planes (~20) with $d_{002} = 0.33$ nm, and all these continuous 002 planes tend to orientate toward the direction of the nanotube-axis.

To provide information about chemical bonding, the nanotubes produced at 1800 °C are analyzed by EELS. The core-level electronic structure was examined by moving the electron probe along a segment perpendicular to the nanotube-axis from the outer surface (Figure 6a) to the center (Figure 6c) and by measuring the excitation edges. Figure 6 clearly shows the presence of the *K*-shell excitations of B (194 eV) and N (400 eV) for typical BN-NTs produced at 1800 °C from the liquid polymeric borazine.

Both π^* and σ^* energy-loss peaks are present, indicating a primary sp^2 bonding character in the BN phase produced at 1800 °C. A comparison with the fine structure obtained from bulk *h*-BN[40] (99.99 atom % from Nilaku Co. Ltd) and with a previous work devoted to the preparation of BN-NTs from pristine carbon.[41] Single wall nanotubes show that resolution features are very similar with no significant shifts in the peak positions. Nevertheless, the analysis shows a change in the intensity ratio between the π^* and σ^* energy-loss peaks going

SCHEME 1. Preparation Process of Ordered Nanotube Arrays[a]

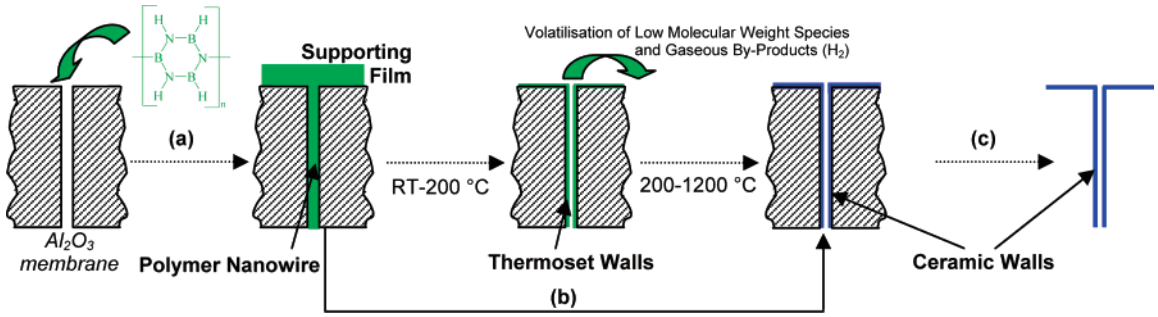

[a] (a) LPI of the membrane with the polymeric borazine, (b) thermolysis process, (c) AAO removal step.

from the outer surface (Figure 6a) to the center (Figure 6c). This is not surprising since the first peak π^* is only allowed for momentum transfers perpendicular to the BN sheet. The cylindrical feature of the nanotube explains why this peak does not totally vanish.

In a more detailed way, the B 1s spectrum of polymer-derived BN-NTs produced at 1800 °C was examined (Figure 7). It exhibits a sharp peak at 194 eV due to the excitonic B 1s $\rightarrow \pi^*$ transition (denoted as 1 in Figure 7a).

The excitonic B 1s$\rightarrow \sigma^*$ transition is represented by the peaks centered at 202, 207, and 218 eV and a shoulder at around 235 eV, denoted as 2, 3, 4, and 5 in Figure 7a, respectively. This particular shape of the excitonic transitions obtained from treated at 1800 °C confirms the sp^2 type of bonding. A comparison made with the spectrum obtained for the BN-NTs prepared at lower temperature, i.e., 1200 °C, where the peaks are not so well-defined (Figure 7b) confirms the significant improvement in the stacking order of layers with the annealing temperature as previously observed by SEM and HRTEM analyses. It should be noticed that a similar assignment can be made for the N K edge spectrum as shown in Figure 8.

In final, it is observed that the nanotubes produced at 1800 °C display a crystalline quality comparable to BN-NTs prepared by CVD, arc-discharge, and laser-ablation methods.[14−18] This result combined with the high chemical purity of polymer-derived BN-NTs is an extremely important advantage for numerous applications. Moreover, in contrast to BN-NTs prepared by other routes, the nanotube model system presented here could be modified at will by tuning the tube dimensions, that is, reducing their diameter and length by controlling the diameter of the pore and thickness of the template, and is not limited by the condition growth. Different polymeric borazine and in-house alumina membranes are currently produced for this purpose. This point is of great importance for numerous studies and applications in the mesoscopic scale.

Furthermore, it is possible to control the crystallinity level of the BN phase with the temperature in order to adjust the physical properties of the corresponding nanotubes. To the best of our knowledge, it is the first time that the preparation of BN-NTs with controlled crystallinity using LPI and thermolysis processes from liquid polymers is reported.

The production of tubular morphologies is attributed to depolymerization of the polymer involving volatilization of low molecular weight species during the polymer-to-ceramic conversion. This can be understood by comparing the measured weight loss with the theoretical one deduced from elemental analyses. Figure 9 shows the thermal decomposition curve obtained in a nitrogen atmosphere for the synthesized polymeric borazine that was immobilized in the confined space of the pore of the AAO templates. At low temperature (RT to 200 °C), 95% of the total weight loss occurs. Correspondingly, the DTG curve displays a very high decomposition rate at a temperature at half-minimum of ~98 °C.

The weight decreases slowly in the range 200−1000 °C to reach a measured total weight loss of 53.2%.

Considering a final composition of $B_{3.0}N_{3.0}$ for the product obtained at 1000 °C, it is shown that the measured weight loss is significantly higher than the theoretical one (17%), indicating evaporation of low molecular weight species. According to the DTG curve profile and the very high weight loss (50.5%) in the temperature range of RT to 200 °C, it can be suggested that evaporation occurs below 200 °C. We postulate that such a phenomenon causes loss of green nanowire integrity during the early stages of the polymer-to-ceramic conversion, producing hollow nanowires after thermolysis to 1200 °C. On the basis of these results, we propose a plausible model (shown in Scheme 1) for the formation of tubular morphologies in the AAO nanochannels.

We believe that, in our experiments, the formation process consists of the following steps: in a first step up to 200 °C, the core of the polymer nanowires shaped inside the nanochannels of the membrane after the LPI process is gradually evaporated, while the interface area connected to the AAO material remains as a result of both the high surface free energy of the alumina membrane and the surface morphology. The polymer/alumina interface solidifies upon heating to form a thin transparent thermoset film covering both the pore walls and the membrane surface. In a second step above 200 °C, the subsequent solid state thermolysis leads to dehydrocoupling of B−H and N−H units, forming cross-links between the polymer chains, i.e., B−N bonds, and then transforms the thin thermoset film into nanotubes roughly parallel to each other and vertically oriented in the AAO template to form an array supported by a BN sheet. After the AAO removal step, a parallel arrangement of nanotubes is produced. It should be mentioned that controlling the inside diameter or correspondingly the wall thickness of these template-synthesized nanotubes remains difficult because evaporation is not controlled during the ceramic conversion.

Conclusion

We have described for the first time a simple and cost-efficient method to synthesize highly ordered BN nanotube arrays from a liquid polymeric borazine using nanoscale template channels. The highly ordered and densely packed BN-NT arrays are potentially important for high-temperature and microfluidic applications as well as catalyst supports and storage materials. Since a wide range of polymeric precursors can be developed, the method described here will be tentatively transposed to other inorganic materials. In addition, the length and diameter of these nanotubes can be controlled at will by

varying the thickness and nanochannel diameter of the template membrane used.

Acknowledgment. The authors thank supporting co-workers Hussein Termoss for the synthesis of the molecular borazine and Hicham Moutaabidd for the polymerization of borazine. We gratefully acknowledge the CTμ (Centre Technologique des Microstructures) of the Université Lyon 1 for access to the SEM apparatus.

Supporting Information Available: SEM images of boron nitride nanotubules. This material is available free of charge via the Internet at http://pubs.acs.org.

References and Notes

(1) Xiong, X.; Mayers, B.T.; Xia, Y. *Chem. Commun.* **2005**, 5013−22.
(2) Shantha, Shankar, K.; Raychaudhuri, A. K. *Mater. Sci. Eng. C* **2005**, *25*, 738−51.
(3) Remskar, M. *Adv. Mater.* **2004**, *16*, 1497−1504.
(4) Xia, Y.; Yang, P.; Sun, Y.; Wu, Y.; Mayers, B.; Gates, B.; Yin, Y.; Kim, F.; Yan, H. *Adv. Mater.* **2003**, *15*, 353−89.
(5) Bechelany, M.; Brioude, A.; Cornu, D.; Ferro, G.; Miele, P. *Adv. Funct. Mater.* **2007**, *17*, 939−43.
(6) Samuelson, L.; Thelander, C.; Björk, M. T.; Borgström, M.; Deppert, K.; Dick, K. A.; Hansen, A. E.; Martensson, T.; Panev, N.; Persson, A. I.; Seifert, W.; Sköld, N.; Larsson, M. W.; Wallenberg, L. R. *Physica E* **2004**, *25*, 313−18.
(7) Liu, H.; Li, Y.; Xiao, S.; Li, H.; Jiang, L.; Zhu, D.; Xiang, B.; Chen, Y.; Yu, D. *J. Phys. Chem. B* **2004**, *108*, 7744−47.
(8) An, L.; Xu, W.; Rajagopalan, S.; Wang, C.; Wang, H.; Fan, Y.; Zhang, L.; Jiang, D.; Kapat, J.; Chow, L.; Guo, B.; Liang, J.; Vaidyanathan, R. *Adv. Mater.* **2004**, *16*, 2036−40.
(9) Yang, P. *MRS Bull.* **2005**, *30*, 85−91.
(10) Yang, W.; Araki, H.; Tang, C.; Thaveethavorn, S.; Kohyama, A.; Suzuki, H.; Noda, T. *Adv. Mater.* **2005**, *17*, 1519−23.
(11) Coleman, J. N.; Khan, U.; Gun'ko, Y. K. *Adv. Mater.* **2006**, *18*, 689−706.
(12) Burda, C.; Chen, X.; Narayanan, R.; El-Sayed, M. A. *Chem. Rev.*, **2005**, *105*, 1025−1102.
(13) Chen, Y.; Zou, J.; Campbell, S. J.; Le Caer, G. *Appl. Phys. Lett.* **2004**, *84*, 2430−32.
(14) Chopra, N. G.; Luyken, R. J.; Cherrey, K.; Crespi, V. H.; Cohen, M. L.; Louie, S. G.; Zettl, A. *Science* **1995**, *269*, 966−67.
(15) Loiseau, A.; Willaime, F.; Demoncy, N.; Hug, G.; Pascard, H. *Phys. Rev. Lett.* **1996**, *76*, 4737−40.
(16) Golberg, D.; Bando, Y.; Eremets, M.; Takemura, K.; Kurashima, K.; Yusa, H. *Appl. Phys. Lett.* **1996**, *69*, 2045−47.
(17) Lourie, O. R.; Jones, C. R.; Bartlett, B. M.; Gibbons, P. C.; Ruoff, R. S.; Buhro, W. E. *Chem. Mater.* **2000**, *12*, 1808−10.
(18) Bourgeois, L.; Bando, Y.; Sato, T. *J. Phys. D* **2000**, *33*, 1902−08.
(19) Possin, G. E. *Rev. Sci. Instrum.* **1970**, *41*, 772−74.
(20) Martin, C. R. *Science* **1994**, *266*, 1961−66.
(21) Zhou, Y.; Li, H. *J. Mater. Chem.* **2002**, *12*, 681−86.
(22) Che, G.; Lakshmi, B. B.; Martin, C. R.; Fisher, E. R.; Ruoff, R. S. *Chem. Mater.* **1998**, *10*, 260−67.
(23) Huber, C. A.; Huber, T. E.; Sadoqi, M.; Lubin, J. A.; Manalis, S.; Prater, C. B. *Science* **1994**, *263*, 800−02.
(24) Liang, W.; Martin, C. R. *J. Am. Chem. Soc.* **1990**, *112*, 9666−68.
(25) Brumlik, C. J.; Martin, C. R. *J. Am. Chem. Soc.* **1991**, *113*, 3174−75.
(26) Klein, J. D.; Herrick, R. D.; Palmer, D.; Sailor, M. J.; Brumlik, C. J.; Martin, C. R. *Chem. Mater.* **1993**, *5*, 902−04.
(27) Charcosset, C.; Bernard, S.; Fiaty, K.; Bechelany, M.; Cornu, D. *DBPBMB* **2007**, *1*, 15−23.
(28) Shelimov, K. B.; Moskovits, M. *Chem. Mater.* **2000**, *12*, 250−54.
(29) Greil, P. *Adv. Engineer. Mater.* **2000**, *2*, 339−48.
(30) Bernard, S.; Weinmann, M.; Gerstel, P.; Miele, P.; Aldinger, F. *J. Mater. Chem.* **2005**, *15*, 289−99.
(31) Duperrier, S.; Gervais, C.; Bernard, S.; Cornu, D.; Babonneau, F.; Balan, C.; Miele, P. *Macromolecules* **2007**, *40*, 1018−27.
(32) (*a*) Pender, M. J.; Sneddon, L. G. *Chem. Mater.* **2000**, *12*, 280−83; (*b*) Pender, M. J.; Forsthoefel, K. M.; Sneddon, L. G. *Pure Appl. Chem.* **2003**, *75*, 1287−94; (*c*) Sneddon, L. G.; Pender, M. J.; Forsthoefel, K. M.; Kusari, U.; Wei, X. *J. Eur. Ceram. Soc.* **2005**, *25*, 91−97.
(33) Cheng, Q. M.; Interrante, L. V.; Lienhard, M.; Shen, Q.; Wu, Z. *J. Eur. Ceram. Soc.* **2005**, *25*, 233−41.
(34) Saulig-Wenger, K.; Cornu, D.; Chassagneux, F.; Ferro, G.; Epicier, T.; Miele, P. *Solid State. Comm.* **2002**, *124*, 157−161.
(35) Saulig-Wenger, K.; Cornu, D.; Chassagneux, F.; Epicier, T.; Miele, P. *J. Mater. Chem.* **2003**, *12*, 3058−61.
(36) Wideman, T.; Sneddon, L. G. *Inorg. Chem.* **1995**, *34*, 1002−3.
(37) Fazen, P. J.; Remsen, E. E.; Beck, J. S.; Carroll, P. J.; McGhie, A. R.; Sneddon, L. G. *Chem. Mater.* **1995**, *7*, 1942−56.
(38) Paine, R. T.; Narula, C. K. *Chem. Rev.* **1990**, *90*, 73−91.
(39) Bernard, S.; Chassagneux, F.; Berthet, M. P.; Cornu, D.; Miele, P. *J. Am. Ceram. Soc.* **2005**, *88*, 1607−14.
(40) Huang, J. Y.; Yasuda, H.; Mori, H. *J. Am. Ceram. Soc.* **2000**, *83*, 403−09.
(41) Fuentes, G. G.; Borowiak-Palen, E.; Pichler, T.; Liu, X.; Graff, A.; Behr, G.; Kalenczuk, R. J.; Knupfer, M.; Fink, J. *Phys. Rev. B* **2003**, *67*, 035429.